

Shear strength analyses of internal diaphragm connections to CFT columns

Liping Kang ^{*1}, Roberto T. Leon ² and Xilin Lu ¹

¹ State Key Laboratory of Disaster Reduction in Civil Engineering,
Tongji University, 1239 Siping Rd. Shanghai 200092, P.R. China

² Via Department of Civil and Environmental Engineering, Virginia Tech,
750 Drillfield Drive, Blacksburg, VA 24061, USA

(Received August 31, 2013, Revised November 06, 2014, Accepted November 07, 2014)

Abstract. Previous theoretical equations for the shear capacity of steel beam to concrete filled steel tube (CFT) column connections vary in the assumptions for the shear deformation mechanisms and adopt different equations for calculating shear strength of each component (steel tube webs, steel tube flanges, diaphragms, and concrete etc.); thus result in different equations for calculating shear strength of the joint. Besides, shear force-deformation relations of the joint, needed for estimating building drift, are not well developed at the present. This paper compares previously proposed equations for joint shear capacity, discusses the shear deformation mechanism of the joint, and suggests recommendations for obtaining more accurate predictions. Finite element analyses of internal diaphragm connections to CFT columns were carried out in ABAQUS. ABAQUS results and theoretical estimations of the shear capacities were then used to calibrate rotational springs in joint elements in OpenSEES simulating the shear deformation behavior of the joint. The ABAQUS and OpenSEES results were validated with experimental results available. Results show that: (1) shear deformation of the steel tube dominates the deformation of the joint; while the thickness of the diaphragms has a negligible effect; (2) in OpenSEES simulation, the joint behavior is highly dependent on the yielding strength given to the rotational spring; and (3) axial force ratio has a significant effect on the joint deformation of the specimen analyzed. Finally, modified joint shear force-deformation relations are proposed based on previous theory.

Keywords: joint behavior; CFT columns; shear capacity; shear deformation mechanism; finite element analysis; shear force-deformation relations

1. Introduction

Concrete filled steel tube (CFT) columns are preferred for high rise buildings in China and many other Asian countries because of their superior seismic performance, ability to carry large bidirectional loads efficiently, and their constructability (Morino and Tsuda 2003). Compared to a reinforced concrete (RC) structure, a structure with CFT columns requires smaller column sections, resulting in more usable space, a critical issue in making high rise building economical. Compared to a steel structure, a structure with CFT columns requires less steel usage while providing larger

*Corresponding author, Ph.D. Candidate, E-mail: kangliping2013@gmail.com

lateral stiffness, another important advantage for high rise structures that are typically controlled by drift under wind loads. Systems based on CFT columns have a number of additional advantages such as prefabrication of large column trees in a well-controlled fabrication environment, quick field bolted connections to girders, and a rapid construction cycle that allows multiple trades to work within a few floors of one another as the building construction progresses.

Connections between steel beams and CFT columns with internal diaphragms, external diaphragms, and through diaphragms are recommended in the Chinese design specifications (CECS 2004). Connections with through diaphragms are the main connection type in Japan, because it is considered to be the most appropriate connection to achieve the strength, stiffness, and ductility required for a moment resisting connection (Elremaily and Azizinamini 2001). However, for fabrication the column needs to be divided into three parts (an upper column, a lower column and a joint region) with the through plates sandwiched between them. This requires extensive welding of thick sections, which results in the need for careful fabrication and inspection. Connections with internal diaphragms are common in the US and Japan because of relatively easier fabrication and less welding involved if the columns are large. Connections with external diaphragms have more application than other two connection types in China. This is probably due to large stiffness and ease of fabrication of this connection type. However, external diaphragm connections require more steel usage and welds, which is not economic in super-high rise building. Moreover, researchers have found that the design capacity of the connection may not be achieved in some cases because of local yielding of the external diaphragms (Zhou 2004).

Compared to external diaphragms or through diaphragm connections, internal diaphragm connections require less steel usage and present better appearance (Fig. 1). These connections are preferred in high rise buildings with mega-columns, considering easy fabrication and an overall cost-effect. In a typical internal diaphragm connection, the beam flanges are connected to the steel tube by full penetration groove welds; the beam webs are bolted/welded to the shop welded plates on the steel tube; and, the internal diaphragms are welded to the steel tube from the inside at the flange locations with full penetration groove welds. In a mega-column, the welders can work inside the column, so the column can be kept continuous. In smaller columns, internal diaphragms are welded to three sides of the steel tube, and then the fourth side of the steel tube is built up to complete the steel tube.

The Chinese specification suggests that the splicing of the columns should be in the middle 1/3 height of the column to avoid stress concentration in the joint area. In the joint, the moment from the beam is transferred to the column by internal diaphragms; the shear force is transferred to the column through bolted connections or welds; and the shear force in the joint area is resisted by the steel tube flanges and webs, internal diaphragms and concrete. Previous experimental studies (Lu *et al.* 2000, Ricles *et al.* 2004, Wang *et al.* 2005) showed that internal diaphragm connections result in excellent seismic performance. However, careful welding or special details are needed in order to prevent brittle fracture in the beam-column connections (Youssef *et al.* 1995, Ricles *et al.* 2004, Latour *et al.* 2011).

The Chinese specification (CECS 2004) provides equations for the shear capacity of joints with internal diaphragms. However, the equations are quite different compared to Japanese specification (AIJ 1991). More research (Zhou 2004, Wu *et al.* 2007) has been done on the joint behavior and various estimations on the shear capacity have been given. While it is important to estimate the joint shear capacity in designing a joint, differences of these equations need to be clarified and the accuracy of these equations needs to be validated. This paper will discuss and compare these equations theoretically, and case studies will also be provided for illustration.

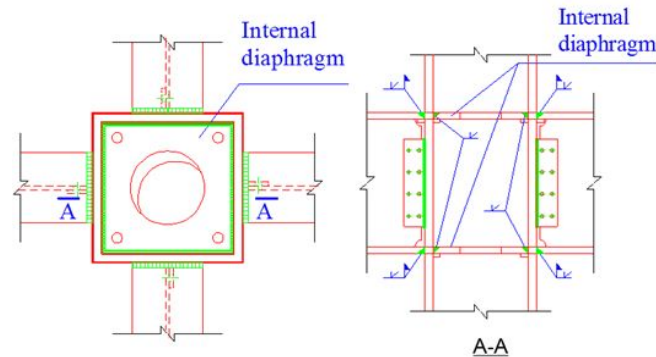


Fig. 1 Connections with internal diaphragms suggested in Chinese code (CECS 2004)

Shear strength has been the main focus of many previous research projects. However, the design of a frame structure requires an accurate prediction of system drift, and this cannot be obtained without a reasonable model for the shear force-deformation of the joint panel zone. The further purpose of this paper is to model the joint behavior between CFT columns and steel beams with internal diaphragms, and study shear force-deformation behavior. This will serve as the first step for development of a comprehensive joint model for design similar to those proposed for other structural types (Lowe and Altoontash 2003, Ibarra *et al.* 2005). The damage mechanism will be discussed and associated nonlinear damage relations will be introduced in this paper. A companion paper describes the case of through diaphragms.

2. Joint behavior

2.1 Joint shear strength

The expressions available in the literature for the shear capacity of the joints (Lu *et al.* 2000, Elremaily and Azizinamini 2001, Zhou 2004, Fukumoto and Morita 2005, Nie and Qin 2007) vary in their assumptions for the shear deformation mechanisms of the joint, in particular with respect to the relative shear capacity ascribed to the concrete and the steel tube. Lu's research (Lu *et al.* 2000), on which the Chinese code (CECS) is based, assumes that two steel tube webs (V_{tw} , calculated from moment resisting capacity of the steel tube webs: M_{tw}) and their welds (V_w , shown as shear strain τ_w in welds), two internal diaphragms (V_{dia} , calculated from moment resisting capacity of the diaphragms: M_{ij}), and the concrete in the joint area (V_{conc}) work together at their nominal design strengths (f_y and f_c) to resist the shear force in the joint (Fig. 2). Most importantly, this approach assumes that their contributions can be added algebraically. This additive approach of simple mechanisms is typical of code approaches for the shear strength design of joints and parallels to those given, for example, for joints between steel beams and concrete columns in AISC 341-10 (AISC 2010).

Three issues need to be clarified with respect to the current Chinese specification approach and to similar design provisions that are analogous to Lu's approach:

- The assumption that the internal diaphragm has reached yield may not be appropriate, because the internal diaphragms are highly restrained by the concrete and the steel tube in

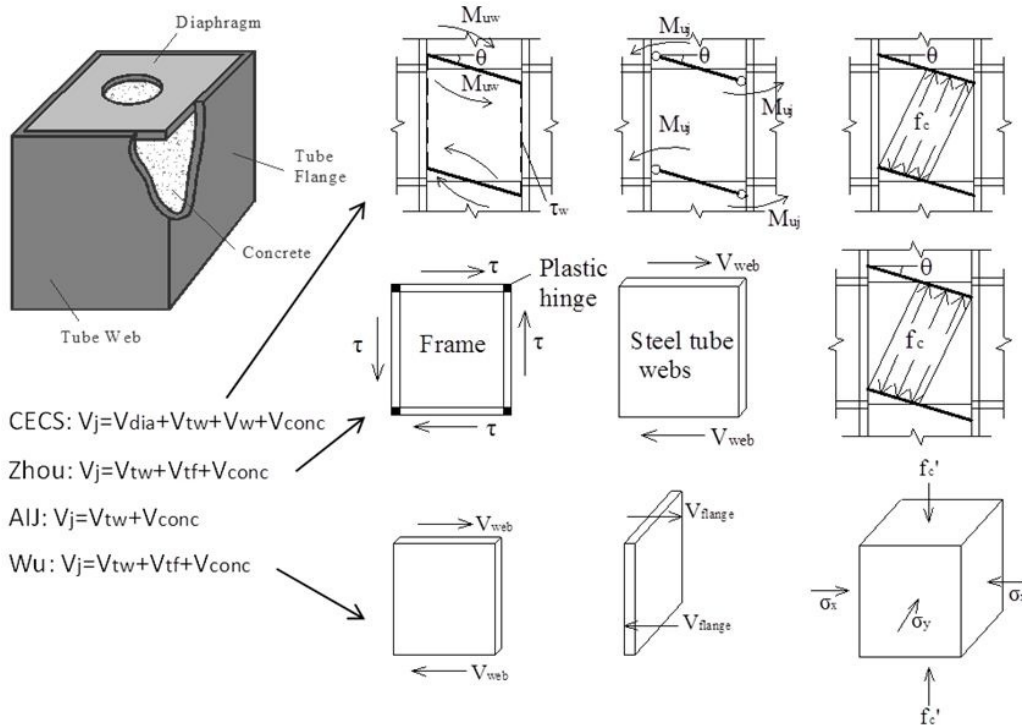


Fig. 2 Contributions of the shear capacity of the joint

the joint area and may not be free to deform and yield as envisioned in a simplified mechanism approach.

- The method does not account for the effect of axial force on the shear capacity of the steel tube or the concrete. It is well-known that there is a shear-axial force interaction particularly for concrete, and the use of mechanisms calibrated for specimens with low or no axial load is not necessarily conservative.
- The welds and the steel tube webs are working in series under shear force, and thus their contribution to the shear capacity should be taken as the smaller one of the two, not as the summation of the two.

Zhou (2004) proposed another simple model to transfer joint shear in which the two steel tube flanges and two internal diaphragms combine to form a “steel frame”, and the two steel tube webs act as a “shear wall”. The “steel frame” (shear strain: τ), “shear wall” ($V_{tw} = 2V_{web}$) and the concrete (V_{conc} , f_c represents the compression force in the concrete, and θ is the shear deformation in the joint) in the joint area act together to resist the shear force (Fig. 2). This model assumes that the “shear wall” yields first, then four plastic hinges appear on the steel tube flanges in the “steel frame”, and finally the concrete reaches its compressive limit and fails. Similar to Lu’s approach, Zhou’s model has some potential problems:

- It takes into consideration the axial force in computing the shear capacity of the steel tube webs, but ignores this effect for the “steel frame”. At least, this appears to be inconsistent.
- The ultimate strength of the steel tube flanges is used in the calculations rather than a

modified nominal value. This approach seems based on the calibration from tests but is inconsistent with compatibility of deformations and inconsistent with the use of yield values elsewhere in the calculations.

- The shear capacity of the concrete is calculated directly from an empirical expression for a steel shape reinforced concrete column connection without consideration of the difference in confinement of the joint. The generality and accuracy of this type of expression is subject to debate.

The Japanese code for composite connections assumes that two steel tube webs and the concrete in the joint work together to resist the shear force in the joint and gives very simple equations (Fig. 2) for the shear capacity of the joint (Morino and Tsuda 2003, AIJ 1991). The issues of this approach are:

- The contribution of the steel tube flanges is not included in the equation; this approach will underestimate the shear capacity of the joint.
- The effect of the axial force on both the capacity of the steel tube webs and the concrete is not considered. This will overestimate the shear capacity of the joint.

Researchers believe that the effects of the two issues mentioned above are of about the same magnitude, thus can cancel each other in the design. This justification cannot be accepted if a correct analysis is desired.

2.2 Joint shear force-deformation relations

All the theories above give the shear capacity but not the related shear deformation of the joint. The shear force-deformation relationship of the panel zone has been studied by several researchers (Fukumoto and Morita 2005, Nie and Qin 2007, Wu *et al.* 2007). The equation proposed by Nie and Qin (2007) provide close estimation of the elastic stiffness of the joint, but the estimations on unloading stiffness and energy dissipation capacity are far off from many experimental results. The equation proposed by Fukumoto and Morita (2005) gives satisfactory estimation of the joint up to the concrete ultimate strength; while underestimates the shear capacity after the concrete reaches its ultimate strength. Wu's equation (Wu *et al.* 2007) is derived from bolted joints to concrete-filled tubes. It assumes that two steel tube webs ($V_{tw} = 2V_{web}$) undergo shear deformation and two steel tube flanges experience flexural deformation ($V_{tf} = 2V_{flange}$) (Figs. 2(a) and (d)) under shear force. The Mohr-Coulomb failure criterion is adopted in this method to evaluate the ultimate shear capacity of the concrete ($V_{conc} = f(f'_c, \sigma_x, \sigma_y)$, f'_c is the compressive force in the concrete, and σ_x, σ_y is the confining force from the steel tube). The writers believe that the shear deformation mechanism of Wu *et al.* (2007) is reasonable and easy to understand. However, this method was derived for bolted connections and validations are needed for its application to welded connections. In this research, Wu's equation will be used to derive shear force-deformation relationship of the welded connections; then the shear force-deformation relationship will be implemented into open software OpenSEES (Mazzoni *et al.* 2007) and compared to experimental data available.

2.3 Joint deformation

The typical deformation of a connection under moment and shear forces (V_b, V_c) is shown in Fig. 3. The deformation of the joint includes a rigid rotation of the joint θ due to elastic and

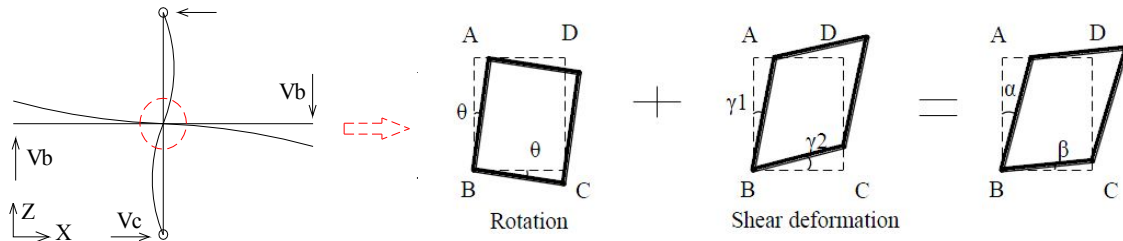


Fig. 3 Deformations of the joint

inelastic flexural deformations in the beams and columns, and the shear deformation γ_1 and γ_2 due to shear force (the positive sign represents a decrease of the angle ABC). The shear deformation of the panel zone γ is

$$\gamma = \gamma_1 + \gamma_2 = \alpha + \beta \quad (1)$$

Where, α and β are the deformation of steel tube flanges (side AB) and internal diaphragms (side BC), respectively.

From a finite element analysis, such as those that can be conducted using ABAQUS (DSSC 2010), the displacements of the nodes at the four corners of the panel zone (node A, B, C, D) are easily obtainable, and the total shear deformation of the joint can be expressed as

$$\gamma = \alpha + \beta = \frac{(dx_A - dx_B) + (dx_D - dx_C)}{2h_b} + \frac{(dz_D - dz_A) + (dz_C - dz_B)}{2h_c} \quad (2)$$

Where, dx_i ($i = A, \dots, D$), dz_i ($i = A, \dots, D$) are the global displacements of each point in the X and Z directions, respectively; h_c is the width of the panel zone; and h_b is the height of the panel zone. This equation will be used to calculate the shear deformation of the joint from ABAQUS analysis, and will be compared to the experimental data available from the literature.

To arrive at simplified expressions for including shear deformation into the design of composite connections, detailed analysis of several test specimens found in the open literature were carried out using ABAQUS. These models served to clarify force transfer mechanisms, address compatibility concerns, and assess concrete effectiveness. Based on these studies, a simplified joint model consisting of several springs was developed and implemented in OpenSEES.

3. ABAQUS analyses of the connections

3.1 ABAQUS models

The purpose of this study is to investigate the effect of diaphragms on the shear capacity of the joint. Five finite element analysis models of connections between steel beams and square CFT columns with internal diaphragms were developed utilizing ABAQUS (Table 1). The YG3, YG4, and YG5 models differ in the concrete strength, steel tube thickness and axial force ratio; and the results are validated with experimental data available from Lu's test (Lu *et al.* 2000). In the test,

Table 1 Specimen details

Specimens	Hollow section of the column $hc \times t$ (mm)	Beam section $hb \times bf \times tw \times tf$ (mm)	Diaphragm thickness td (internal diameter) (mm)	Axial load N (kN)	Concrete grade
YG3	200 × 5	260 × 100 × 5 × 5	6 (Φ70)	0.4N0 (900)	C50
YG4	200 × 4	260 × 100 × 5 × 5	6 (Φ70)	0.2N0 (900)	C40
YG5(BASE)	200 × 4	260 × 100 × 5 × 5	6 (Φ70)	0.4N0 (900)	C50
NOD	200 × 4	260 × 100 × 5 × 5	N/A	0.4N0 (900)	C50
2TD	200 × 4	260 × 100 × 5 × 5	10 (Φ70)	0.4N0 (900)	C50

constant axial force was applied on the top of the column, and cyclic loading was applied on each beam end. The YG5 (BASE), NOD and 2TD models differ in the diaphragms details: the NOD model has no diaphragms; the BASE model has 6 mm thick diaphragms and the 2TD model has 10 mm thick diaphragms. Monotonic analyses in ABAQUS were compared to the cyclic analyses in the test due to difficulty in modeling damage in the highly confined concrete in the joint under cyclic loading. Validation of the structural behavior with monotonic loading using cyclic test results is reasonable because the YG3, YG4, and YG5 connection tested by Lu showed stable hysteresis characteristics and little deterioration with cycling loading (Lu *et al.* 2000).

Model with symmetrical boundary conditions was created in ABAQUS in order to save computational memory and time. Previous analyses (Hu 2008) have proved that this technique is reliable and cost-effective. The models were composed of several independent parts including steel tubes, concrete, beams and internal diaphragms, as shown in Fig. 4. Three dimensional eight nodes brick element with full integration and incompatible modes (C3D8I) were adopted for all the parts above. A finer meshing was used in the joint area in order to capture the complex stress distribution (Fig. 4). A total of 5362 nodes and 3132 elements were used.

Steel meeting the Chinese Q235 specification (essentially equivalent to an ASTM A36 in strength and ductility) was used in the test and the strength of the steel material was varied with the thicknesses of the steel plates. A bilinear stress-strain relationship with a strain hardening of 1% was adopted for all the steel materials. The material strength varied slightly depending on the thickness of the steel tubes (4 mm or 5 mm), beams (5 mm) and diaphragms (6 mm) and a 0.2% strain offset was initially considered to be the yield stress as Q235 does not have a clear yield point as true A36 would have. The yield stress was increased by 10% in the ABAQUS final analyses in order to better representing the real constitutive model of the steel.

The constitutive models for the concrete incorporated the confinement from the steel tube calculated utilizing the approach from Han (2004), in which the coefficient of restrain effect from the steel tube to concrete is used. The concrete damaged plasticity model in ABAQUS was used; this model accounts for tension stiffening of the concrete. Only the tensile damage factor was utilized in the model in order to avoid convergence problem caused by the crushing of the concrete. As there is very limited slippage between the concrete and the steel tube in the joint area because the concrete is capped by two internal diaphragms, the effect of the slippage between the concrete and the steel tube on the overall behavior of the connection is small. Thus a “tie constraint” was used between the concrete and the steel tube along the whole height of the steel tube in the BASE and 2TD model. Even though the NOD model has no diaphragms, the “tie constraint” is still adopted; so the only difference among these three models is the diaphragm thickness. Similarly

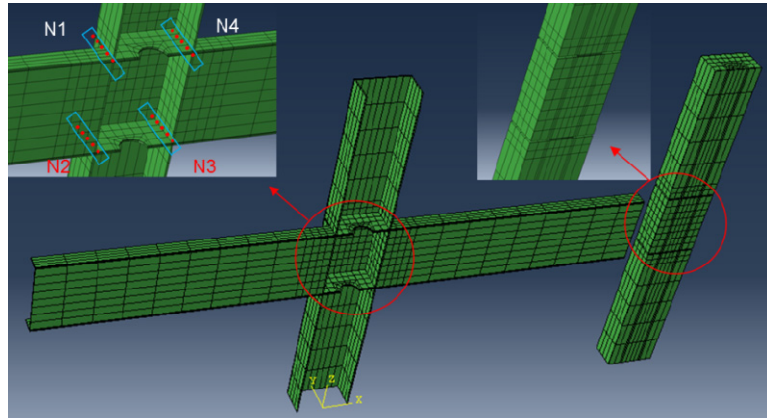


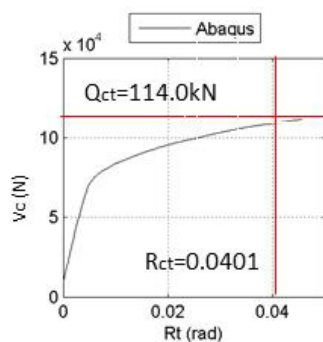
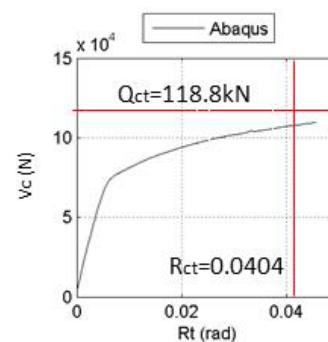
Fig. 4 ABAQUS model of the BASE model

both the concrete and the diaphragms and the beam and internal diaphragms were tied to the steel tube.

A pressure P was applied at the top of the column to represent the axial force N in the first step, and lateral displacements Δ_b were applied on the nodes at both beam ends in the second step.

3.2 ABAQUS model validations

The story shear force (shear force acting on column end, V_c)-story drift rotation (R_i) relations of the YG3, YG4, and YG5 model are compared to the test in Figs. 5-7 (the story shear force-story drift rotation curve for YG5 is given, while only maximum strength and related rotation of YG3 and YG4 are provided in the literature). The model provides close simulation on the maximum strength ($Q_{ct} = 114.0$ kN for YG3, $Q_{ct} = 118.8$ kN for YG4) and related story drift rotation ($R_{ct} = 0.0401$ radians for YG3 and $R_{ct} = 0.0401$ radians for YG4) for YG3 and YG4 model. The loading was only in positive direction in ABAQUS analyses, but the negative portion is plotted as symmetrical in order to get a full sight into the comparison for YG5 (BASE) model (Fig. 7). The ABAQUS model gives close estimation of the BASE model in the light of initial stiffness and strength. The shear force (V_j)-deformation (γ) relation of the joint in the BASE connection is

Fig. 5 V_c - R_t curve of the YG3 connectionFig. 6 V_c - R_t curve of the YG4 connection

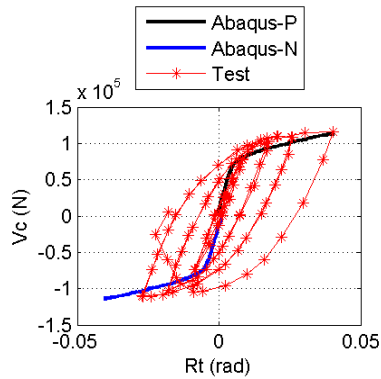


Fig. 7 V_c - R_t curve of the BASE connection

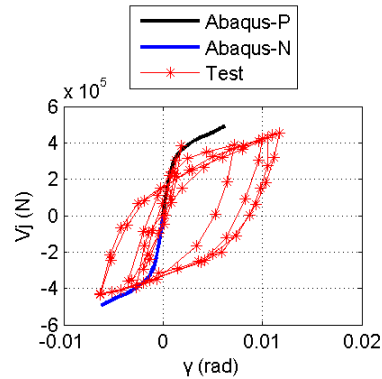


Fig. 8 V_j - γ curve of the joint in BASE connection

shown in Fig. 8 (shear deformation of the joint is calculated from Eq. (2)). The estimated shear deformation is close to that in the test for most of the load history, while the shear deformation localizes in the positive direction in the last two cycles in the test. It shows that the ABAQUS model gives satisfactory simulations to the test results with varies parameters including concrete strength, steel strength, steel tube thickness and axial force ratio.

3.3 ABAQUS results

This section mainly discusses analyses results for YG5 (BASE), NOD, and 2TD models to investigate the effect of diaphragms on shear strength and deformation of the joint.

3.3.1 Plastic strain distributions

The plastic strain distribution in the joint area is studied to obtain a visual insight of the force transfer path and possibly provide a potential yielding mechanism of the joint. Fig. 9 shows the plastic strain (Max PE) distribution in the beams at a story drift rotation angle of 0.035 radians (NOD model fails to converge after 0.035 radians). The plastic strain is concentrated in a very small area of the beam in the NOD model (Fig. 9(a)). It is distributed over a larger area in the BASE model (Fig. 9(b)) with a local strain concentration at the flange corner (see the red circle in

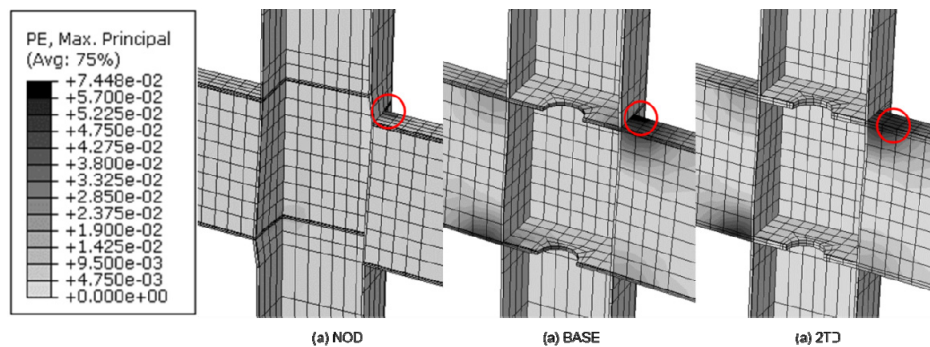


Fig. 9 Maximum principal strain in the beam

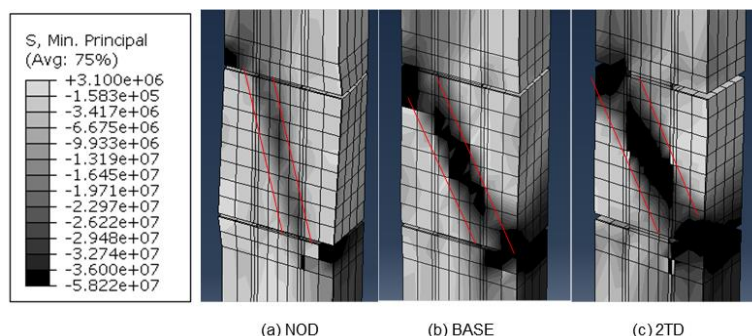


Fig. 10 Minimum principal stresses of the concrete in the joint

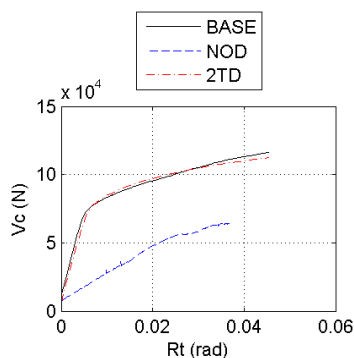
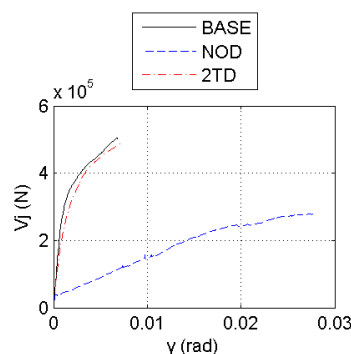
Fig. 11 V_c - R_t curveFig. 12 V_j - γ curve

Fig. 9(b)). The plastic strain distributed uniformly over the entire flange width of the beam in the 2TD model (see the red circle in Fig. 9(c)). This shows that the stiffening effect of the diaphragms leads to a more distributed force transferring mechanism as the thickness of the diaphragms increases.

Fig. 10 shows the minimum principle stresses of the concrete in the joint at the story drift rotation angle of 0.035 radians. Compared to the stresses in the NOD model (Fig. 10(a)), the stress distribution shows a clear compression strut in the concrete both in the BASE and 2TD models (Figs. 10(b)-(c)). Compared to the BASE model, the compression strut covers a wider and more complete path in the 2TD model (see the area between red lines). This indicates that the diaphragms have a significant influence in confining the concrete in the joint; the confining area increases with the increase of the diaphragm thickness.

3.3.2 Shear capacities

The story shear force of the 2TD model (107.7 kN) at $R_t = 0.035$ radians is close to that of the BASE model (109.6 kN), while the shear capacity of the NOD model (63.9 kN) is only about 58.3% of that in the BASE model (Fig. 11). The shear deformation in the joint of the 2TD model at $R_t = 0.035$ radians (0.0054 radians) is close to that of the BASE model (0.0056 radians), while the shear deformation of the joint in the NOD model (0.0263 radians) is 4.7 times that of the BASE model (Fig. 12). The shear deformation component of the joint is further shown in Fig. 13. It is obvious that shear deformation components α and β of the 2TD model are close to those of the

BASE model, leading to very similar resultant shear deformations γ in both specimens (Figs. 13(b)-(c)). However, the shear deformation α of the NOD model is much larger than that of the BASE model, and the shear deformation component β has the same sign (both positive sign), leading to a much larger shear deformation than the BASE model (Fig. 13(a)).

The force transferred through diaphragms and the relative deformation of two steel tube flanges are shown in Fig. 14 (in order to compare, the diaphragms in the NOD model simply refer to the concrete at the location of the internal diaphragms in the BASE model). The force transferred through the “concrete diaphragm” of the NOD model (61.5 kN) is only around 36.5% of that in the BASE model (166.6 kN) at $R_t = 0.035$ radians because of different force transferring mechanisms between concrete and steel diaphragms. The force transferred through the diaphragms in the 2TD model (161.6 kN) is close to that in the BASE model. This shows that the steel diaphragms transfers force efficiently from the beam flanges to the column; increasing of the thickness of the diaphragms does not make a significant difference in the force transferred.

The comparison shows that the internal diaphragms increase both the shear strength and stiffness of the joint; this is achieved by forcing the two steel tube flanges to deform as one body in the joint. However, this increase of strength and stiffness has a limit. Further increasing the

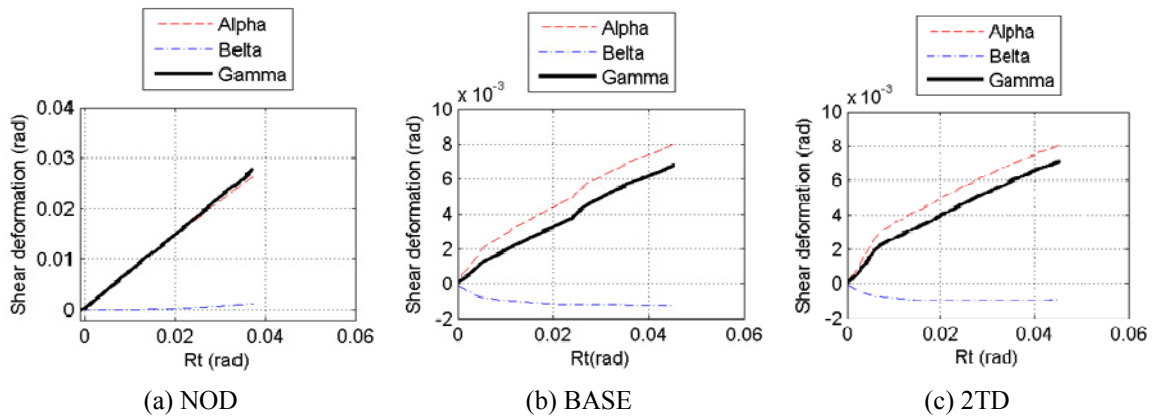


Fig. 13 Component deformations of the joint

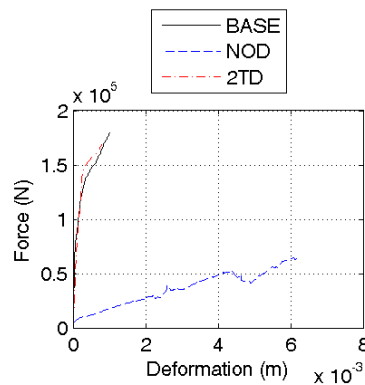


Fig. 14 Forces transferred through diaphragms

diaphragm thickness (from 6 mm to 10 mm) does not have a significant increase on the strength or stiffness of the connection.

4. OpenSEES analyses of the connections

As noted in the introduction, previous researchers have made different assumptions about the applicable shear deformation mechanism of the joint. This results in different equations for calculating the shear strength contribution of the steel tube and the concrete. In this section, the shear capacity from different theories are calculated and compared to the ABAQUS analyses. Then, models are created in OpenSEES to analyze the effect of the shear force-deformation relation of the joint on the overall behavior of the joint and the connection (Fig. 15). The OpenSEES model utilizes “NonlinearBeamColumn” fiber elements for both the column and the beam. In the joint, zero length translational springs are used to simulate the column-joint (GS1 and GS2), and beam-joint (GS3 and GS4) connections, and a zero length rotational spring (R1) is used to represent the shear mechanism in the shear panel zone. An “Elastic” material with high stiffness (1.0×10^{10} N/m) is used for the springs at column-joint connections, and beam-joint connections to simulate perfect welded connections. A “steel02” material was used for the shear force-shear deformation curve for the rotational spring in the joint; this relationship was obtained from the ABAQUS analyses or Wu’s equation and was transformed into a moment-rotation relationship.

4.1 Shear capacity from available theories

The estimated shear capacity contributions of each component (steel tube webs, steel tube flanges, internal diaphragm, concrete, etc.) are calculated in this study for BASE, NOD and 2TD connections based on available theories including AIJ, CECS, Wu and Zhou. The contributions are normalized by dividing 6.68×10^5 N (shear capacity of the joint calculated from CECS) for convenient comparison, shown in Table 2. The authors believe that the welds should not be considered in CECS equation and the estimated shear capacity of the panel zone without the weld

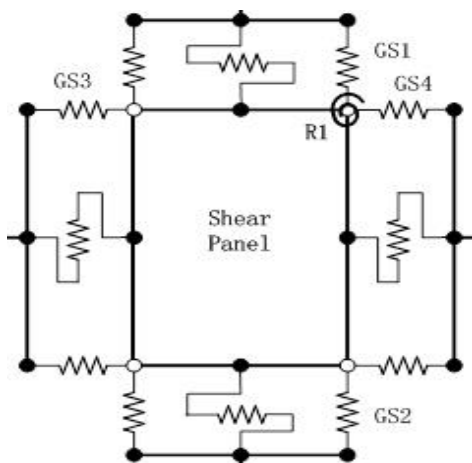


Fig. 15 Connection model in OpenSEES

Table 2 The shear capacity of the connections with internal diaphragms (BASE, NOD and 2TD)

Specimens	Theories	Steel tube webs /welds	Steel tube flanges /internal diaphragms	Concrete	Joint
BASE	AIJ	0.380	0.000	0.645	1.025
	CECS	0.599	0.010 ^a	0.391	1.000
	CECS-m	0.219	0.010 ^a	0.391	0.620
	Zhou	0.329	0.005 ^b	0.747	1.084
	Wu	0.365	0.003 ^b	0.293	0.662
NOD	AIJ	0.380	0.000	0.645	1.025
	CECS	0.599	0.000	0.391	0.990
	CECS-m	0.219	0.000	0.391	0.609
	Zhou	0.329	0.005 ^b	0.747	1.084
	Wu	0.365	0.003 ^b	0.293	0.662
2TD	AIJ	0.380	0.000	0.645	1.025
	CECS	0.599	0.029 ^a	0.391	1.018
	CECS-m	0.219	0.029 ^a	0.391	0.638
	Zhou	0.329	0.005 ^b	0.747	1.084
	Wu	0.365	0.003 ^b	0.293	0.662

Note: ^a contribution from internal diaphragms; ^b contribution from steel tube flanges

contribution is also listed in the table (see CECS-m). Take the BASE model for example, the calculated shear capacities of the joint from AIJ (1.025), CECS (1.000) and Zhou (1.084) are close; while Wu's estimation (0.662) is around 66% of the former. The total shear capacity of the joint is comparable from different theories; however, the contribution from each component is far off. CECS equation takes into account contributions from steel tube webs, welds, and concrete: the contribution from steel tube webs and welds (0.599) is more significant over concrete (0.391); while the diaphragms contribution is only 0.01. AIJ equation only considers shear strength contribution from concrete and steel tube webs, and the concrete contribute a more significant part (0.645) over steel tube webs (0.380). Zhou's equation includes shear strength from steel tube webs, steel tube flanges, and the concrete; while the concrete shear strength (0.747) is more than two times of the steel tube webs (0.329); steel tube flanges only contribute 0.005. In Wu's equation, the contribution of the concrete (0.293) and steel tube webs (0.365) are close, while steel tube flanges shear strength is only 0.003. The reason for different component contribution is that each theory assumes different deformation mechanisms and adopts different methods of calculating the shear strength of each component.

The estimated shear capacities of NOD and 2TD models are the same as BASE model from AIJ, Zhou, or Wu estimations because the diaphragms have no shear contributions in these three theories. According to CECS equation, diaphragms contribute 1% of the joint shear strength in BASE model; while they contribute around 3% (0.029/1.018) of the joint shear strength in 2TD model. While it seems from the CECS equation that the diaphragms may contribute a significant part in the shear strength, the calculation shows that the shear strength contribution of the diaphragms is negligible. Because of this reason, the calculated shear strength of the NOD model

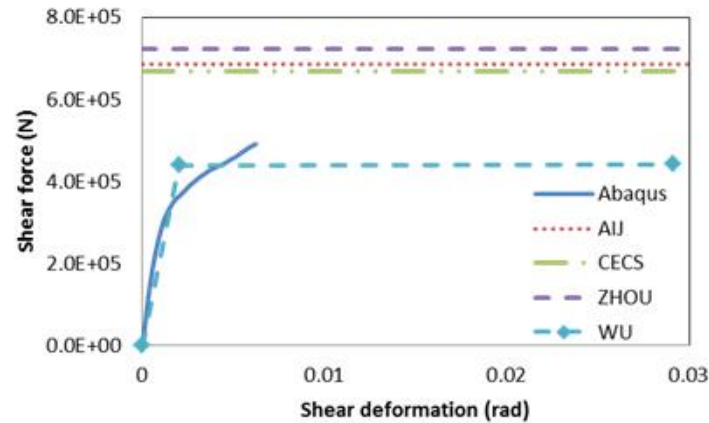


Fig. 16 Shear capacity of the BASE connection

Table 3 Shear capacity of the SCP and SCC connections

Specimens	Theories	Steel tube webs /welds	Steel tube flanges /internal diaphragms	Concrete	Joint
SCP	AIJ	0.305	0.000	0.102	0.407
	CECS	0.428	0.024 ^a	0.046	0.498
	CECS-m	0.124	0.024 ^a	0.046	0.194
	Zhou	0.278	0.003 ^b	0.117	0.399
	Wu	0.283	0.003 ^b	0.058	0.363
SCC	AIJ	0.662	0.000	0.084	0.747
	CECS	0.066	0.024 ^a	0.046	1.000
	CECS-m	0.269	0.024 ^a	0.046	0.338
	Zhou	0.562	0.014 ^b	0.094	0.670
	Wu	0.566	0.014 ^b	0.051	0.651

is only 1% less than the BASE connection, and that from 2TD connection is only 2% higher than the BASE connection from CECS theory. This serves a proof that the thickness of the diaphragm has a very limited effect on the shear capacity of the joint. The shear capacity of the BASE model is further compared to the ABAQUS estimation in Fig. 16. Wu's equation has a close estimation on the initial stiffness of the joint compared to ABAQUS simulation.

The difference of these theories is extensively studied by calculating shear strength of other two connections tested by Morino *et al.* (1993). The thickness of the steel tube in the joint area of SCC connection is two times of that in SCP connection. Their shear strength is listed in Table 3. All the values are divided by 7.22×10^5 N for convenient comparison, which is the shear capacity of the joint in SCC connection calculated from CECS equations. It is seen that the joint shear strength of the SCC connection is almost two times of SCP connection from each theory; steel tube webs and concrete contribute most of the shear strength for the joint, while shear strength contributions from steel tube flanges/internal diaphragms are negligible.

4.2 Shear capacity of the joint from ABAQUS analyses

A bilinear curve is adopted to simulate the shear force-deformation relationship curve from ABAQUS analysis. This relationship is then transformed to a moment-rotation relationship and is used to calibrate the rotational spring in the panel zone in OpenSEES analysis for the BASE connection. It is seen that the story shear force-story drift rotation relations from OpenSEES analyses are in good agreement with the ABAQUS analysis and the test result in terms of the strength and stiffness (Fig. 17(a)) of the connection. The model also gives reasonable estimation of the shear deformation of the joint (Fig. 17(b)). The larger shear deformation in the test may due to loss of stability in the last cycle.

4.3 Shear capacity of the joint from Wu's equation

An OpenSEES analysis utilizing the joint deformation mechanism from Wu's was also conducted for the BASE connection. The model results in a good simulation of the overall strength and stiffness of the connection (Fig. 18(a)). However, the joint mainly stays in the elastic range in

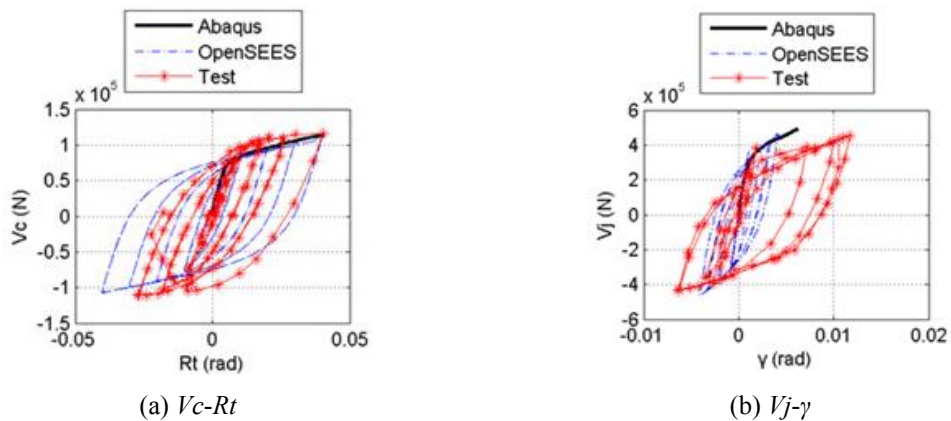


Fig. 17 OpenSEES results with joint behavior obtained from ABAQUS analyses for the BASE connection

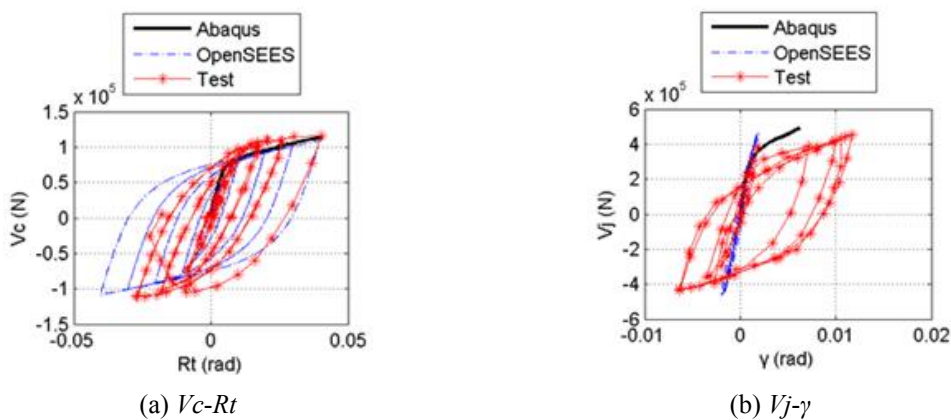


Fig. 18 OpenSEES results with joint behavior obtained from Wu's equation for the BASE connection

the OpenSEES analyses and experiences very limited deformation (-0.002~0.002 radians for the last cycle), while the joint reaches plastic range and experiences large plastic deformation (-0.006~0.011 radians for the last cycle) in the tests. It is obvious that Wu's equation underestimates the shear deformation of the joint. This result illustrates one of the problems of blindly utilizing models with concentrated springs; while the overall results may appear reasonable, the individual contributions may be completely off.

5. Modified shear force-deformation relations of the joint

5.1 Shear force-deformation relations of the joint

From the shear deformation results from the ABAQUS analyses, the “ α type deformation” (shown in Fig. 2) is dominant for BASE, NOD, and 2TD connections (Fig. 13). The analyses show that the yielding of the steel tube flanges and webs corresponds to the point where major yielding of the joint occurs. A comparison of the BASE connection and the 2TD connection shows that the thickness of the diaphragms does not have a significant effect on the shear strength of the joint. This would imply that the diaphragms do not directly contribute to the shear capacity of the joint. However, the analyses shows that deformation of the steel tube flanges should be considered in the shear deformation mechanism. Thus the shear deformation mechanism of Wu's method rather than that from CECS method is more appropriate for these connections. Wu's approach gives good estimation for the story shear force-drift story rotation relationship of the BASE connection, but underestimates the shear deformation in the joint. Thus modifications should be made to Wu's approach in order to better simulate these connections.

Wu's equation assumes that the yielding mechanism of the joint experiences four stages (Wu *et al.* 2007): (1) The concrete “yields” first because of its low shear strength compared to the steel tube; (2) Next, the concrete reaches its ultimate shear strength; (3) Then the steel webs yield; (4) Finally, four plastic hinges occur in steel flanges, and the joint reaches its ultimate strength. While it is a common knowledge that the shear capacity of the steel tube will decrease under axial force; this effect was negligible in Wu's calculation. Wu's equation does not consider the effect of the axial force ratio on the shear capacity of the steel tube, which gave satisfactory estimations on experiments conducted. However, the effect of neglecting this decrease on joint simulations (rotational spring) in OpenSEES needs to be verified.

5.2 OpenSEES verifications

Shear capacity of the BASE connection (axial force equals to 0.4) is recalculated with the consideration of the axial force ratio effect in Wu's equations. The complete (four stages) shear force-deformation relationship of the joint is shown in Fig. 19. The calculated relation in Fig. 19 serves as verification on the assumption of the yielding order of each component in the joint. The four stage shear force-deformation relation gives a close estimation of the stiffness compared to ABAQUS results. Meanwhile, estimated shear capacity of the joint from the modified method is 6% lower than Wu's estimation, as a result of taking into consideration of the effect of axial force on the steel tube.

The model for the BASE joint was implemented in OpenSEE with the joint behavior calculated from the modified formulas. However, a bilinear relationship instead of the four lines curve of the

joint was adopted to represent the joint behavior in the OpenSEES analyses for simplicity. In the last cycle (Fig. 20), the simulated shear deformation is 0.018 radians (-0.010~0.008 radians), compared to the test result 0.017 radians (-0.006~0.011 radians). The result shows that the modified formula gives a close estimation both on the global behavior of the connection and the shear deformation of the joint.

5.3 Discussions of the axial force ratio on the column

A noticeable phenomenon is that, the shear capacity of the joint in the BASE connection from the proposed formula is only 6% less than the estimation from Wu. However, the shear deformation from the proposed formula is close to the test results while that from Wu is much smaller. This is because the yielding shear force of the joint is around 4.2×10^5 N from ABAQUS analyses. The estimated yielding strength from Wu is 4.41×10^5 N, so the joint stays in the elastic range (Fig. 20(b)) under loading; while the estimated yielding force from the proposed formula is 4.16×10^5 N, and the joint experiences plastic deformation under the loading. This shows that the simulation of the shear deformation of the joint highly depends on the yielding strength given to

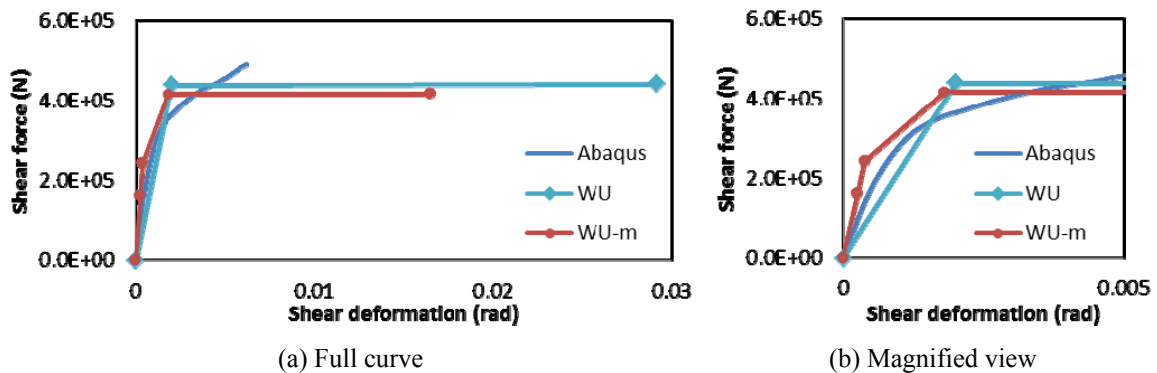


Fig. 19 Shear force-shear deformation curves of the joint from the proposed equation (BASE model)

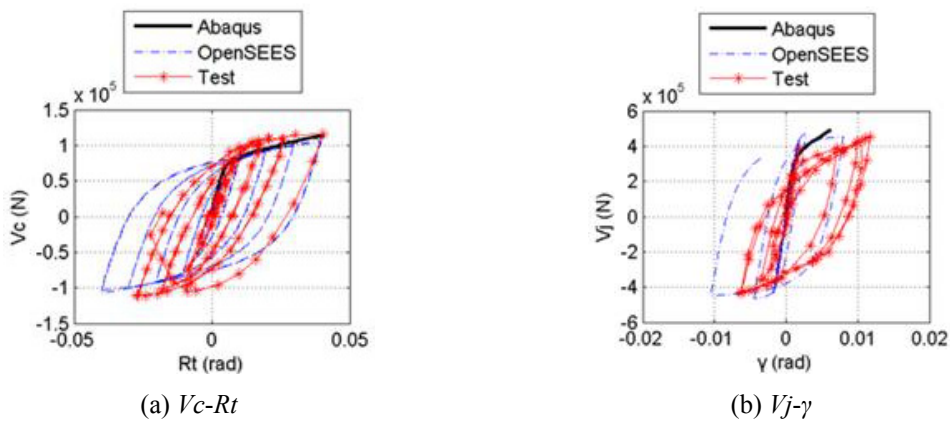


Fig. 20 OpenSEES results of the BASE connection with proposed formula for the joint

the rotational spring. Neglecting the axial force ratio has a minor effect on the shear strength of the joint, while it has a significant influence on the simulated shear deformation of the joint in the case of joint yielding.

6. Conclusions

Finite element analyses are conducted in ABAQUS to investigate the damage behavior of the internal diaphragm connections to CFT columns with experimental validations from literature. ABAQUS results show:

- The existence of the diaphragms increases both the strength and stiffness of the connection. However, this increase has a limit. Further increasing the thickness of the diaphragms does not have a significant effect on the overall behavior of the connection.
- The deformation of the steel tube flanges (α type deformation) in the joint area other than the diaphragms (β type deformation) dominates the shear deformation of the joint.

The shear force-deformation relations of the joint are obtained from ABAQUS analyses and compared to the shear capacities calculated from previous theories. While these theories give various estimations on the shear capacities of the joint, one common feature is that concrete and steel tube webs contribute most of the joint shear strength and the contributions from steel tube flanges or diaphragms are negligible. Wu's equation is found to be more appropriate for estimating shear strength of diaphragm connections.

OpenSEES analyses on these connections are then conducted with the joint behavior obtained from ABAQUS or Wu's estimation. The results show that:

- The OpenSEES model with joint behavior from ABAQUS analyses gives a close simulation to the connection.
- The simulation of the OpenSEES model with joint behavior from Wu's equation has a satisfactory estimation on the overall behavior of the connection while underestimates the shear deformation of the joint.

The damage mechanism of the joint with considerations of the axial force effect is introduced and then is used in OpenSEES analyses. The model gives satisfactory simulation both on the overall behavior of the connection and the shear deformation of the joint. Considerations of the axial force ratio have a significant effect on the joint behavior analyzed.

While conclusions are given based on analyses conducted herein, more validations are needed to verify the shear deformation mechanism of the joint, especially the α/β type deformation. Besides, more experiments are needed to establish a reasonable and reliable shear strength-deformation relation of the joint.

References

- AIJ (1991), *Standard for Structural Calculation of Steel Reinforced Concrete Structures*, Architectural Institute of Japan.
- AISC (2010), *Seismic Provisions for Structural Steel Buildings*, AISC, Chicago, IL, USA.
- CECS (2004), *Technical Specification for Structures with Concrete-filled Rectangular Steel Tube Members*,

- China Engineering Construction Standardization Association, Beijing, China. [In Chinese]
- DSSC (2010), *Abaqus 6.10 Analysis User's Manual*, Dassault Systems Simulia Corp., Providence, RI, USA.
- Elremaily, A. and Azizinamini, A. (2001), "Design provisions for connections between steel beams and concrete filled tube columns", *J. Construct. Steel Res.*, **57**(9), 971-996.
- Fukumoto, T. and Morita, K. (2005), "Elastoplastic behavior of panel zone in steel beam-to-concrete filled steel tube column moment connections", *J. Struct. Eng.*, **131**(12), 1841-1853.
- Fukumoto, T. and Morita, K. (2005), "Elastoplastic behavior of panel zone in steel beam-to-concrete filled steel tube column moment connections", *J. Struct. Eng.*, **131**(12), 1841-1853.
- Han, L.H. (2004), *Concrete Filled Steel Tube Structures-Theory and Practice*, Science Press of China, Beijing, China. [In Chinese]
- Hu, J.W. (2008), "Seismic performance evaluations and analyses for composite moment frames with smart SMA PR-CFT connections", Ph.D. Thesis; Georgia Institute of Technology, Atlanta, GA, USA.
- Ibarra, L.F., Medina, R.A. and Krawinkler, H. (2005), "Hysteretic models that incorporate strength and stiffness deterioration", *Earthq. Eng. Struct. Dyn.*, **34**(11), 1489-1511.
- Latour, M., Piluso, V. and Rizzano, G. (2011), "Cyclic modeling of bolted beam-to-column connections: Component approach", *J. Earthq. Eng.*, **15**(4), 537-563.
- Lowes, L.N. and Altoontash, A. (2003), "Modeling reinforced-concrete beam-column joints subjected to cyclic loading", *J. Struct. Eng.*, **129**(12), 1686-1697.
- Lu, X.L., Yong, Y., Kiyoshi, T. and Satoshi, S. (2000), "Experimental study on the seismic behavior in the connection between CFRT column and steel beam", *Struct. Eng. Mech., Int. J.*, **9**(4), 365-374.
- Mazzoni, S., McKenna, F., Scott, M.H., Fenves, G.L. et al. (2007), *OpenSEES Command Language Manual*, Department of Civil Environmental Engineering, University of California, Berkeley, CA, USA.
- Morino, S., Kawaguchi, J., Yasuzaki, C. and Kanazawa, S. (1993), "Behavior of concrete-filled steel tubular three-dimensional subassemblages", *Proceedings of an Engineering Foundation Conference, ASCE*, Potosi, MO, June, pp. 726-741.
- Morino, S. and Tsuda, K. (2003), "Design and construction of concrete-filled steel tube column system in Japan", *Earthq. Eng. Eng. Seismol.*, **4**(1), 51-73.
- Nie, J.G. and Qin, K. (2007), "Research on shear performance of concrete-filled square steel tubular column connections", *J. Build. Struct.*, **28**(4), 8-17. [In Chinese]
- Ricles, J.M., Peng, S.M. and Lu, L.W. (2004), "Seismic behavior of composite concrete filled steel tube column-wide flange beam moment connections", *J. Struct. Eng.*, **130**(2), 223-232.
- Wang, L., Wang, T. and Deng, P. (2005), "Experimental research on seismic performance of joint reinforced with inner ring stiffener of concrete-filled square tubular frame", *Earthq. Eng. Eng. Vib.*, **25**(1), 76-80.
- Wu, L.-Y., Chung, L.-L., Tsai, S.-F., Lu, C.-F. and Huang, G.-L. (2007), "Seismic behavior of bidirectional bolted connections for CFT columns and H-beams", *Eng. Struct.*, **29**(3), 395-407.
- Youssef, N.F.G., Bonowitz, D. and Gross, J.L. (1995), "A survey of steel moment-resisting frame buildings affected by the 1994 Northridge earthquake", National Institute of Standards and Technology; US Department of Commerce.
- Zhou, T.H. (2004), "Study on seismic behavior and load-carrying capacity of concrete-filled square tubular column to steel beam connection", Xi'an University of Architecture and Technology, Xi'an, China. [In Chinese]